Control of a Fluidized Bed Polyethylene Reactor

Vahidi, Omid; Shahrokhi, Mohammad*+
Department of Chemical and Petroleum Engineering, Sharif University of Technology, P.O. Box 113659465 Tehran, I.R. IRAN

Mirzaei, Ahmad
Iran Polymer and Petrochemical Institute, Faculty of Polymerization Engineering, Tehran, I.R. IRAN

ABSTRACT: *In present paper, dynamic behavior and control of a fluidized bed reactor for polyethylene production has been considered. A double active sites model for Ziegler-Natta catalysts is used for simulation of polymerization reaction. Hydrodynamic behavior of the bed is modeled using a two phase model including bubble and emulsion phases in which bubble phase has plug flow pattern with differentially variable velocity and size through the bed and emulsion phase has the CSTR flow pattern. The reactor model is validated using industrial data. Conventional PID controllers with anti-windup are considered for control purposes. It has been shown that the control system has satisfactory performances either for setpoint tracking or load rejection. To improve the performance of the control system for load rejection the cascade control strategy has been considered.*

KEY WORDS: *Fluidized bed reactor, Polyethylene, PID control, Dynamic simulation, Two phase model.*

INTRODUCTION

Nowadays polyethylene is considered to be the world largest produced polymer in petrochemical plants. Because of the advantages of gas-phase processes such as moderate reaction operating conditions, absence of solvent and well mixing of the components, production of different grades of polyolefin in the fluidized bed reactor (FBR) has been recognized as one of the most efficient processes for olefin polymerization in petrochemical plants. Recently modeling and simulation of polyethylene production in a fluidized bed reactor has received considerable attention.

Choi and *Ray* [1] proposed a two phase model including bubble and emulsion phases with constant bubble size. *McAluey et al.* [2] proposed a single phase model by modifying the Ray's model with additional assumptions. In a comparison between two models, they have shown that the single phase assumption doesn't make considerable difference in the results obtained from the models. *Hatzantonis et al.* [3] in a research work developed the two phase model by considering the bubble growth effect on hydrodynamic behavior of the reactor and have shown that the developed model has a better

* *To whom correspondence should be addressed.*
+ *E-mail: Shahrokhi@sharif.edu*
1021-9986/08/3/87 15/$/3.50

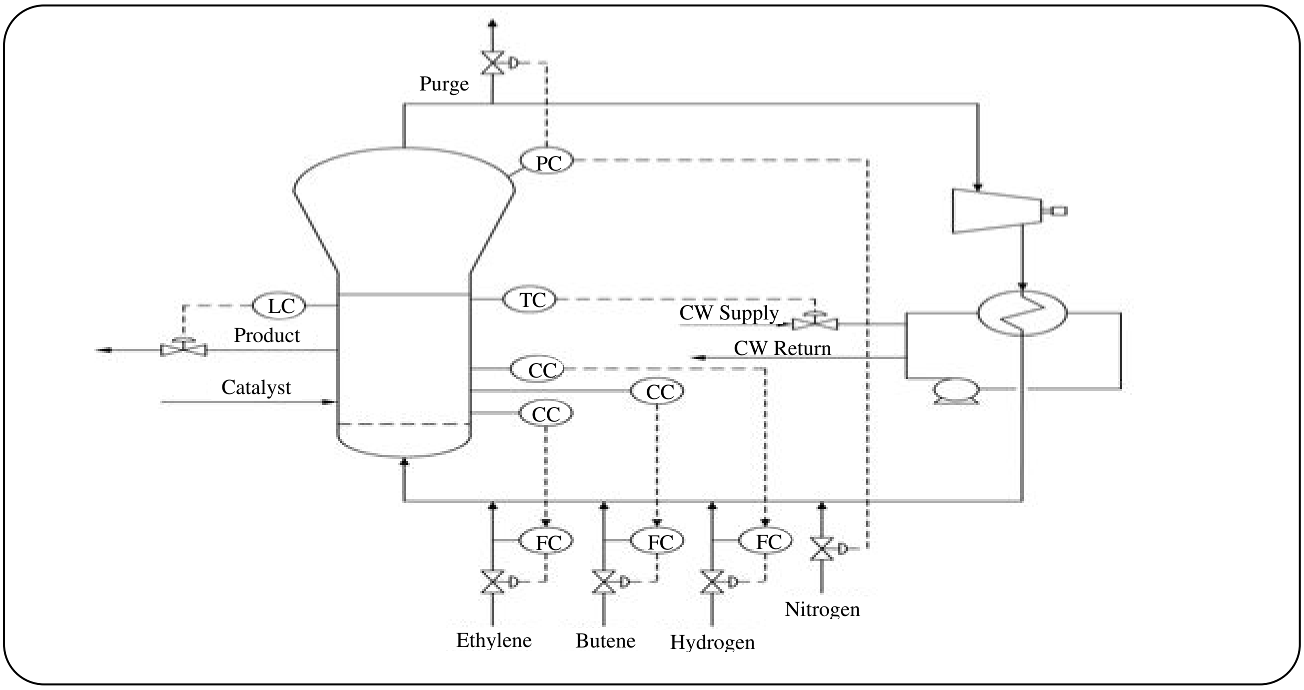

Fig. 1: Schematic flow diagram of a polyethylene production process using FBR.

agreement with industrial data than single and two phase model with constant bubble size. In another work, *Kiashemshaki et al.* [4] developed the two phase model by considering the polymerization reaction not only in the emulsion phase but also in the bubble phase. They have indicated that about 20 % of the polymerization reaction occurs in bubble phase.

In this work a two phase model including bubble and emulsion phases which considers the bubble growth effect is used for modeling the hydrodynamic behavior of the reactor. The double active sites Ziegler-Natta catalyst model proposed by *McAuley et al.* [5] has been used for simulating the kinetic of ethylene copolymerization. To control the reactor at the operating conditions, six feedback control loops with PID controllers, including anti-windup, have been used. The advantage of the present work over the previous ones is considering dynamic for the bubble phase in dynamic simulation of the reactor.

In the previous works a simple CSTR model has been used for dynamic simulation and control, while we have used a comprehensive two phase model for control purposes. To improve the performance of the control system for load rejection, cascade control strategy has been implemented. Simulation results indicate that this strategy promotes the control performance considerably.

The paper has been organized as follows. First reactor modeling is discussed. Next reactor dynamic and its control have been considered. Finally the simulation results are presented and discussed.

REACTOR MODELING

A schematic representation of a gas-phase ethylene copolymerization FBR is depicted in Fig. 1. As can be seen from Fig. 1, a gas stream comprises four components (ethylene, 1-butene, hydrogen and nitrogen) is fed continuously to the reactor through a distributor. Catalyst particles are introduced to the reactor above the distributor. Polymer particles produced in the reactor are withdrawn from middle of the reactor. Because of the low conversion, the unreacted gas leaving the reactor is recycled to the reactor. Since the polymerization reaction is exothermic, an external heat exchanger is employed for cooling the recycle gas stream.

The following assumptions are made for modeling the reaction loop:

1- Emulsion phase is perfectly mixed and stays in the minimum fluidization condition.

2- Polymerization reaction occurs only in the emulsion phase.

3- Bubble phase has plug flow pattern and its properties change differentially through the bed.

4- No elutriation of solids occurs.

5- Heat and mass transfer resistances between solid and gas phases are negligible.

6- Solid particles have an average size.

The reactor modeling is accomplished in two sections. In the first section the polymerization reaction modeling is discussed and in the second section reactor hydrodynamic modeling is considered.

Polymerization reaction modeling

In the present study, a comprehensive model proposed by *McAuley et al.* [5] is considered to describe the ethylene copolymerization kinetics over the Ziegler-Natta catalyst. This model is based on the theory of catalyst with double active sites. Table 1 shows the mechanism of the copolymerization kinetics.

Table 1: Ethylene 1-butene copolymerization kinetics mechanism over Ziegler-Natta catalyst.

Activation by cocatalyst	$S_p^j + C \xrightarrow{kf^j} N_0^j$
Initiation	$N_0^j + M_i \xrightarrow{ki_i^j} N_{1,i}^j$
Propagation	$N_{r,i}^j + M_k \xrightarrow{kp_{ik}^j} N_{r+1,k}^j$
Transfer to monomer	$N_{r,i}^j + M_k \xrightarrow{ktm_{ik}^j} N_{1,k}^j + D_r^j$
Transfer to hydrogen	$N_{r,i}^j + H_2 \xrightarrow{kth_i^j} N_{0,H}^j + D_r^j$
Reinitiation	$N_{0,H}^j + M_i \xrightarrow{kih_i^j} N_{1,i}^j$
Transfer to cocatalyst	$N_{r,i}^j + C \xrightarrow{ktc_i^j} N_{1,1}^j + D_r^j$
Spontaneous transfer	$N_{r,i}^j \xrightarrow{kts_i^j} N_0^j + D_r^j$
Spontaneous deactivation	$N_{r,i}^j \xrightarrow{kds^j} N_d^j + D_r^j$
Spontaneous reactivation	$N_d^j \xrightarrow{kas^j} N_0^j$

Reactor dynamic modeling

To model the reactor dynamics, mass and energy balances are derived for each phase to obtain concentrations of monomers and other components, reactor temperature and average molecular properties of the copolymer.

Bubble phase modeling

The molar balance for each component in an axial element yields:

$$\frac{\partial([M_i]_b\delta)}{\partial t} = -\frac{\partial(U_b[M_i]_b\delta)}{\partial z} - Km_i([M_i]_b - [M_i]_e)\,\delta \quad (1)$$

$$i = 1,2,.....,n$$

where the second term in right side of the equation is the rate of mass transfer between emulsion and bubble phases. The energy balance for an axial element gives:

$$\frac{\partial\left(\sum_{i=1}^{n}[M_i]_b Mw_i Cp_i \delta T_b\right)}{\partial t} = \quad (2)$$

$$-\frac{\partial\left(\sum_{i=1}^{n}[M_i]_b Mw_i Cp_i \delta(T_b - T_{ref})U_b\right)}{\partial z} - \sum_{i=1}^{n} Km_i([M_i]_b -$$

$$[M_i]\,)Mw_i Cp_i \delta(T_b - T_{ref}) - Hm_{av}(T_b - T_e)\,\delta$$

where the second term in right side of the equation is the rate of heat transfer as a result of mass transfer and the third term is the heat transfer between two phases. In reference [3], above equations in the steady state form have been used and accumulation terms in bubble phase are neglected.

Emulsion phase modeling

From the molar balances of the monomers, hydrogen and nitrogen we have [3]:

$$\frac{d([M_i]_e V_e)}{dt} = U_{e-in}[M_i]_{in}(1-\delta_{in})\,\varepsilon A - \quad (3)$$

$$U_{e-o}[M_i]_e(1-\delta_o)\,\varepsilon A + \int_0^H Km_i([M_i]_b - [M_i]_e)\,\delta A dz -$$

$$Q\varepsilon[M_i]_e - R_{M_i}V_p \qquad i = 1,2$$

$$\frac{\partial([M_{H_2}]_e V_e)}{\partial t} = U_{e-in}[M_{H_2}]_{in}(1-\delta_{in})\,\varepsilon A - \quad (4)$$

$$U_{e-o}[M_{H_2}]_e(1-\delta_o)\varepsilon A + \int_0^H Km_{H_2}([M_{H_2}]_b - [M_{H_2}]_e)\,\delta A dz -$$

$$Q\varepsilon[M_{H_2}]_e - R_{H_2}V_p$$

$$\frac{d([M_{N_2}]_e V_e)}{dt} = U_{e-in}[M_{N_2}]_{in}(1-\delta_{in})\,\varepsilon A - U_{e-o}[M_{N_2}]_{in}(1-\delta_o)\,\varepsilon A + \int_0^H Km_{N_2}([M_{N_2}]_b - [M_{N_2}]_e)\delta A dz - Q\varepsilon[M_{N_2}]_e \quad (5)$$

where "Q" denotes the volumetric flow rate of gas and polymer mixture withdrawn from the reactor and R_{M_i} and R_{H_2} are consumption rates of monomers and hydrogen respectively and are obtained from following equations [5]:

$$R_{M_i} = \sum_{j=1}^{s}[M_i]Y_0^j Kp_{Ti}^j \qquad i = 1,2,...,m \quad (6)$$

$$R_{H_2} = \sum_{j=1}^{s}[H_2]Y_0^j Kth_T^j \quad (7)$$

$Y\nu$ is the νth moment of the live polymer chains and is given by [5]:

$$Y_\nu^j = \sum_{i=1}^{m}\sum_{r=1}^{\infty} r^\nu [N_{r,i}^j] \quad (8)$$

The third term in equations (3)-(5) shows the total amount of mass transfer between bubble and emulsion phases. The mass balance for solid particles existing in the bed yields [3]:

$$\frac{d(\rho_p V_p)}{dt} = q_{cat} - (1-\varepsilon)\rho_p Q + \left(\sum_{i=1}^{m} R_{M_i} Mw_i + R_{H_2} Mw_{H_2}\right)V_p \quad (9)$$

where "q_{cat}" denotes the inlet catalyst mass flow rate. From the above equation V_p is calculated. Having the emulsion phase voidage, the emulsion phase volume, V_e, is obtained. The volume of the bubble phase, V_b, can be calculated by solving the bubble phase equations. From V_e and V_b the total bed volume is determined. Dividing the bed volume by the bed cross-section, area the bed height is calculated.

The energy balance for emulsion phase results in [3]:

$$\frac{d(\sum_{i=1}^{n}[M_i]_e Mw_i Cp_i T_e V_e + \rho_p Cp_p T_e V_p)}{dt} = \quad (10)$$

$$\sum_{i=1}^{n}[M_i]_{in} Mw_i Cp_i U_{e-in}(1-\delta_{in})\varepsilon A(T_{in} - T_{ref}) - \sum_{i=1}^{n}[M_i]_e Mw_i Cp_i U_{e-o}(1-\delta_o)\varepsilon A(T_e - T_{ref}) - \sum_{i=1}^{m} R_{M_i} Mw_i \Delta H_i V_p + \int_0^H Hm_{av}(T_b - T_e)\delta A dz + \int_0^H \sum_{i=1}^{n} Km_i([M_i]_b - [M_i]_e) Mw_i Cp_i \delta A(T_b - T_{ref})dz - Q(1-\varepsilon)\rho_p Cp_p(T_e - T_{ref}) + q_{cat}Cp_p(T_{in} - T_{ref}) - \sum_{i=1}^{n}[M_i]_e Mw_i Cp_i Q\varepsilon(T_e - T_{ref})$$

Since the temperature variation in the reactor is small, its effect on the heat capacity has been neglected while the effect of composition has been taken into account. Correlations needed to calculate the parameters used in above equations are given in the Table 2.

Assuming lump formulation for the external heat exchanger, the heat balance on tube side of the heat exchanger yields:

$$\frac{d(T_g \rho_g Cp_{g-av})}{dt} = \frac{\dot{m}_{rec} Cp_{g-av}(T_{g-in} - T_g) - U_{ex}A_{ex}(T_g - T_w)}{V_{tube}} \quad (11)$$

and heat balance on shell side of the heat exchanger results in:

$$\frac{d(T_w)}{dt} = \frac{\dot{m}_w Cp_w(T_{w-in} - T_w) + U_{ex}A_{ex}(T_g - T_w)}{\rho_w Cp_w V_{shell}} \quad (12)$$

where subscripts "g", "w" and "ex" denote recycle gas, cooling water and heat exchanger respectively.

The polymer density and melt index (MI) can be calculated in terms of cumulative polymer composition and weight-average molecular weight [5]. The instantaneous polymer composition can be calculated in terms of monomer consumption rates as follows:

$$\varphi_i = R_i / \sum_{i=1}^{m} R_i \quad (13)$$

where "R_i" is the consumption rate of monomer i. The symbol "φ_i" denotes the instantaneous mole percent of

Table 2: Correlations used for calculating the required parameters [6].

$K_m = (\frac{1}{K_{bc}} + \frac{1}{K_{ce}})^{-1}$	Overall mass transfer coefficient
$K_{bc} = 4.5(\frac{U_{mf}}{d_b})5.85(\frac{D_g^{1/2} g^{1/4}}{d_b^{5/4}})$	Bubble-cloud mass transfer coefficient
$K_{ce} = 6.77\left(\frac{D_g \varepsilon_{mf} U_n}{d_b}\right)^{1/2}$	Cloud-emulsion mass transfer coefficient
$H_m = H_{bc} = 4.5\left(\frac{U_{mf}\rho_g C_{pg}}{d_b}\right) + 5.85\frac{(k_g \rho_g C_{pg})^{1/2} g^{1/4}}{d_b^{5/4}}$	Overall heat transfer coefficient
$\delta = \frac{U_0 - U_{mf}}{U_b}$	Bubble phase volume fraction
$U_{mf} = \frac{Re_{mf} - \mu_g}{\rho_g - d_p}$	Minimum fluidization velocity
$Re_{mf} = (28.7^2 + 0.0494Ar)^{0.5} - 28.7$	Reynolds number
$Ar = \frac{d_p^3 \rho_g (\rho_S - \rho_g) g}{\mu_g^2}$	Archimedes number
$d_b = d_{bm} - (d_{bm} - d_{b0})\exp\left(-\frac{0.3z}{D}\right)$	Bubble diameter
$d_{bm} = 0.652[A(U_0 - U_{mf})]^{0.4}$	Maximum bubble diameter
$d_{b0} = 0.00376(U_0 - U_{mf})^2$	Initial bubble diameter
$U_b = U_0 - U_{mf} + 0.711(gd_b)^{0.5}$	Bubble rise velocity
$U_e = \frac{U_{mf}}{\varepsilon_{mf}(1-\delta)}$	Emulsion gas velocity

monomer i in polymer. By solving the following equation cumulative polymer composition can be calculated.

$$\frac{d(\rho_p \Phi V_p)}{dt} = \dot{m}_{p-in}\Phi_{i-in_i} + \sum_{i=1}^{m} R_{M_i} Mw_i V_p \varphi_i - Q(1-\varepsilon)\rho_p \Phi \quad (14)$$

The polymer density can be related to polymer composition by the following equation [5]:

$$\rho_p = a_1 + a_2 \Phi_2^{a_3} \quad (15)$$

where a_1, a_2 and a_3 are parameters calculated offline using measurements of polymer density and polymer composition.

REACTOR CONTROL SYSTEM

Because of the high nonlinearity involved in polymerization reactions and the strong interaction between the reactor variables and also due to instability of reactor operating conditions, control of polymerization reactions in a FBR has been known as a difficult task. However, there are relatively little works on the control of gas-phase polymerization of ethylene in fluidized-bed reactors. Most of these works are limited to the reactor temperature stability and control (*Choi & Ray* [1]; *Dadebo et al.* [7]; *Ali et al.* [8]; *Seki et al.* [9]). McAuley and *McGregor* [10] have studied control of the polymer quality through manipulating the feed flows and have compared the performances of a linear internal model controller (IMC) and a nonlinear feedback controller.

In another work, *Ali et al.* [11] have investigated control of the reactor temperature and pressure in addition to the gas partial pressures. They have compared the performances of two different multivariable control approaches. Recently *Chatzidoukas et al.* [12] have studied the optimal grade transition problem and selection of appropriate pairings for polyethylene production in a FBR.

For process safety and operability, the reactor temperature and pressure as well as the bed height should be controlled at desired operating points. Regarding the product quality, the components concentration (i.e. ethylene, 1-butene and hydrogen concentrations) must be controlled at desired values.

To control the process variables given above, seven manipulated variables are considered. These manipulated variables are the volumetric flow rates of makeup streams (ethylene, 1-butene and hydrogen), nitrogen volumetric flow rate, volumetric flow rate of purge stream, the cooling water makeup mass flow rate and the polymer withdrawal mass flow rate. The control pairings are shown in the Fig. 1 and are given in Table 3.

For each control loops, conventional PID controllers are used. To avoid deterioration of controller performance, the anti-windup scheme which stops integration upon input saturation has been used [13]. Tuning of the controller parameters are accomplished based on maximum 10 % overshoot for each loop while the other loops are open. To handle the loop interactions, the detuning procedure proposed by *Luyben* [14] has been used. Equation describing the flowrate of the gas stream control valve is given below:

$$F = Kv\sqrt{P_{up}(P_{up} - P_{down})} \tag{16}$$

where "F" denotes the volumetric flow rate of gas passing through the valve, "P_{up}" and "P_{down}" denote the upstream and downstream pressures of the gas and "Kv" denotes the valve coefficient which is a function of valve opening.

RESULTS AND DISCUSSION

In this section static and dynamic simulations using the comprehensive model are considered. System model contains 5 partial differential, 37 ordinary differential equations and many algebraic equations used for calculating the various model parameters. To solve this set of equations, backward difference method is used to discretize the partial differential equations with respect to reactor length. The resulting ordinary differential equations are solved using Runge Kutta method through the MATLAB software. The flowchart that represents the solution procedure is shown in Fig. 2.

Static simulation

To check the accuracy of the model, a static simulation has been performed. Program inputs are: rates of each component makeup, pressure difference across the compressor, catalyst and production rates, purge gas and cooling water flow rates. The corresponding figures used for simulation are given in Table 4. These data have been selected such that the feed condition entering the reactor to be the same as an industrial case. The operating condition of gas entering the bed is given in Table 5.

The results of static simulation and the corresponding industrial data are given in Table 6. As can be seen the results of the simulation are in a good agreement with industrial data.

Static simulation can be used for evaluating the effect of different parameters on the reactor performance. As an example, the effect of gas superficial velocity for various catalyst feed rate on emulsion phase temperature and ethylene concentration are shown in Fig 3. In this figure the concentration of ethylene is denoted by C2. As can be seen, increasing the gas superficial velocity results in a better heat removal from the reactor. Therefore the catalyst feed rate can be increased for more production rate without the risk of polymer meld-down. On the other hand, increasing the gas superficial velocity leads to lower conversion of the monomer (Fig. 3). In addition, it can increase the rate of polymer particles elutriation.

Dynamic simulation

Through dynamic simulation, the performances of different control strategies are evaluated for load rejection and set-point tracking. Table 7 shows the desired values of the controlled variables of an industrial polyethylene production unit (Tabriz petrochemical, in the north part of Iran).

Load rejection

In industrial plants a common disturbance is fluctuation of feed stream pressure. Therefore a disturbance is introduced into the all feed stream pressures.

Table 3: The control pairings.

Controlled variable	Manipulated variable
Ethylene concentration	Ethylene makeup feed rate
1-butene concentration	1-butene makeup feed rate
Hydrogen concentration	Hydrogen makeup feed rate
Temperature	Cooling water makeup feed rate
Pressure	Nitrogen and bleed rates
Bed height	Polymer withdrawal rate

Table 4: Program input data.

Makeup $_{Et}$ = 3623.6 g/s	Production = 3722.2 g/s
Makeup $_{Bu}$ = 524.58 g/s	$\Delta P_{compressor}$ = 0.77 bar
Makeup $_{H2}$ = 4.17 g/s	C.W. = 8.396e5 g/s
Makeup $_{N2}$ = 144.5 g/s	dp = 0.1145 cm
Bleed = 0.002*Recycle	ε = 0.5
Prepolymer = 49.72 g/s	

Table 5: Entering gas operating condition.

U_{gas} = 47.6 cm/s	y_{Et} = 0.458
P = 20.77 bar a	y_{Bu} = 0.196
T = 44.6 °C	y_{H2} = 0.097

Table 6: Simulation results and the corresponding industrial data.

	Industrial data	Two phase model
T (°C)	76	75.6
P (bar a)	20.0	20.03
Mw_{pol}	9.7e4	11.2e4
ρ_{pol} (g/cm3)	0.920	0.916
H (cm)	1400	1400

Table 7: The desired values of controlled variables.

$[C_2]=3.163e^{-4}$ mol/cm^3	T= 76 °C
$[C_4]=1.49e^{-4}$ mol/cm^3	P = 20 bar
$[H_2]=7.48e^{-4}$ mol/cm^3	H = 14 m

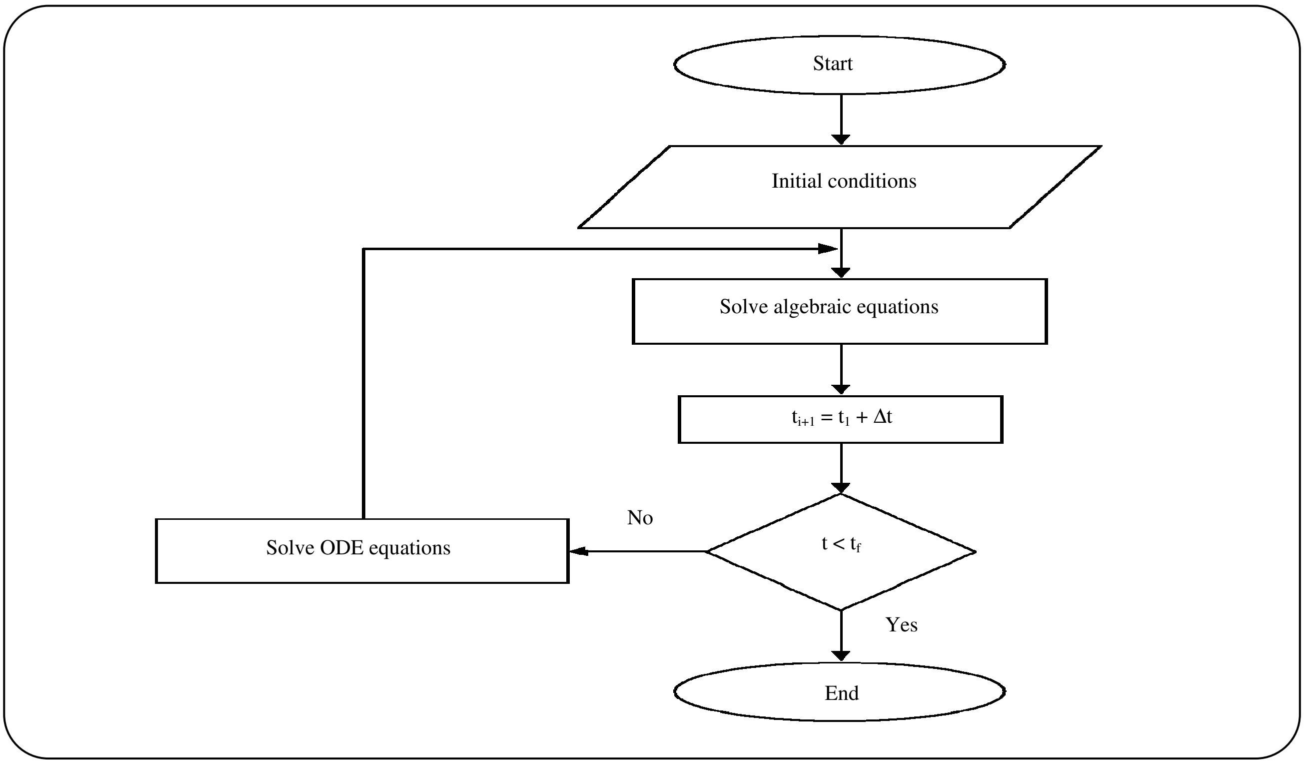

Fig. 2: Flowchart for solving the system equations.

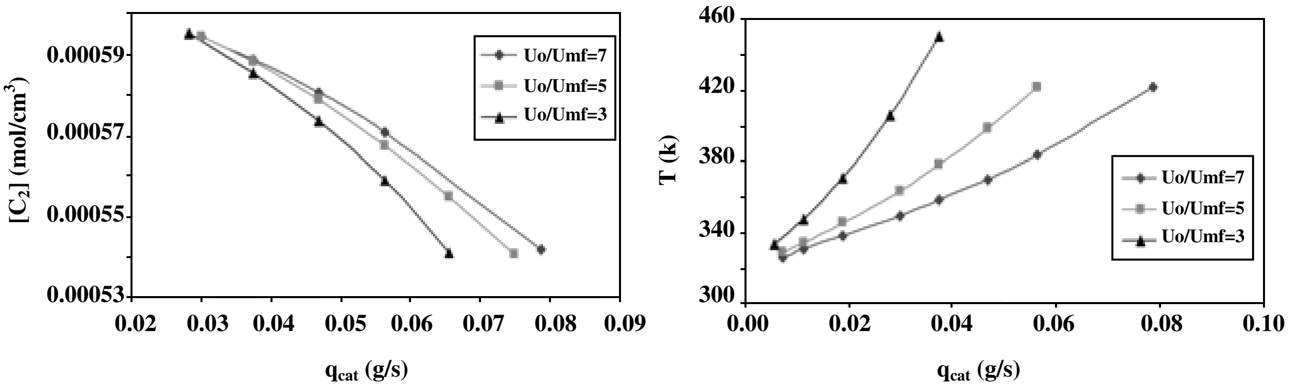

Fig. 3: Variations of emulsion phase temperature and ethylene concentration versus catalyst feed rate.

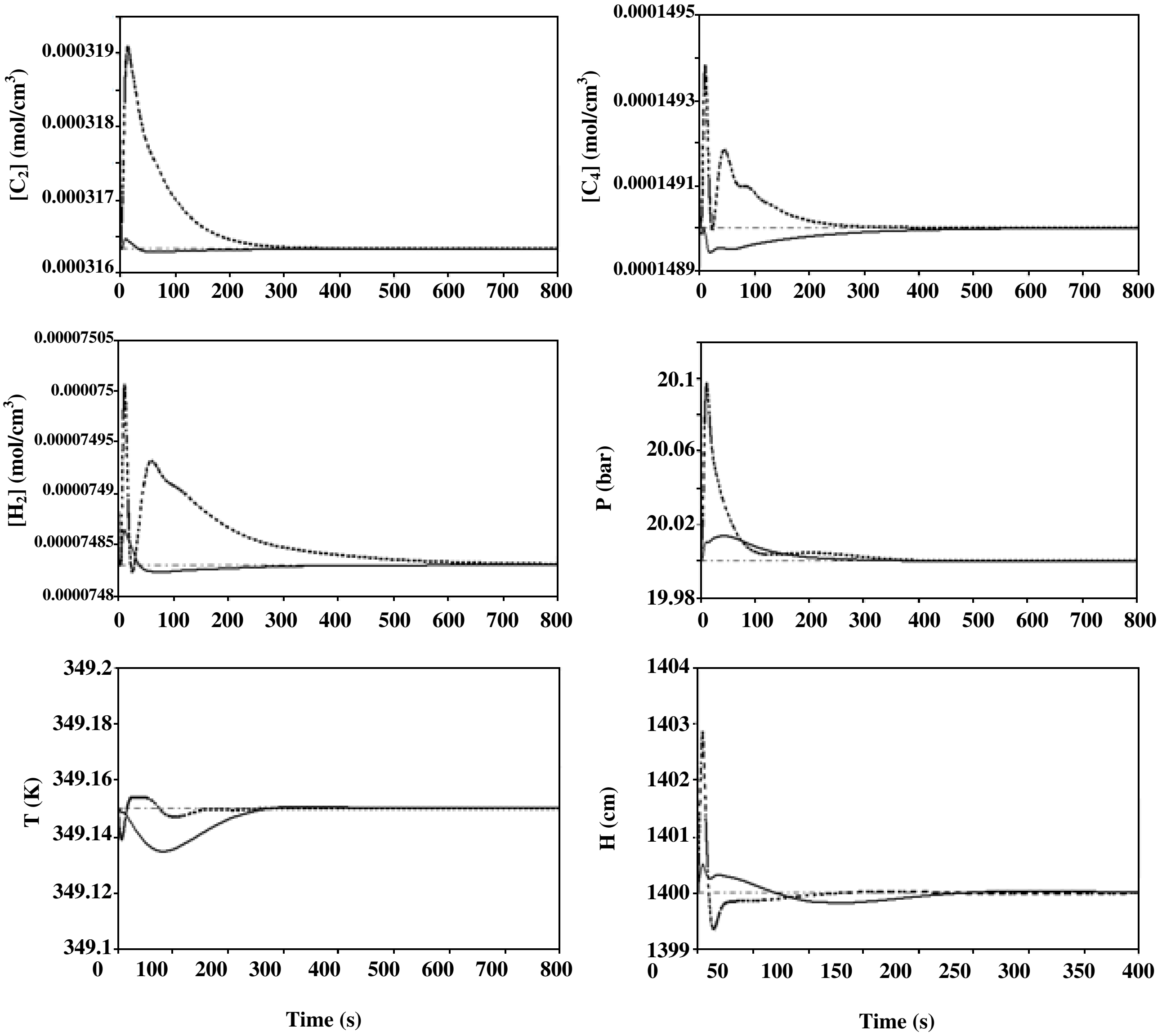

Fig. 4: Deviations of the controlled variables from their steady state values due to 5 bar increase in the makeup stream pressures (---- single concentration loops, —— cascade loops).

Fig. 4 shows the deviation of the controlled variables from their steady state values due to 5 bar increase in makeup stream pressures for single and cascade loops. In this figure the concentration of 1-butene is denoted by C4.

As can be seen, in spite of the large magnitude of the disturbance, deviations of controlled variables from their desired values are small for both control systems but the performance of cascade strategy is superior. This is due to inner loop action which damps the effect of disturbance. Fig. 5 shows the variations of manipulated variables based on valve opening percentage.

As can be seen from Fig. 5 the steady state values of the manipulated variables are not the same for these two cases. The reason is the different values of the purge stream rate under the steady state condition. If the purge rate is fixed and only the nitrogen flow rate is used for controlling the reactor pressure, the steady state conditions for both cases will be the same. To check the dynamic of the system under the fixed purge flow rate, (267 g/s) the same disturbance is introduced to the system keeping the purge rate constant. The results are shown in Figs. 6 and 7. As can be seen all manipulated variables have converged to the same values for the two control strategies.

Setpoint tracking

In this section the desired value of the reactor temperature is increased by 2 centigrade degrees. Fig. 8 shows variations of the reactor temperature and cooling water makeup stream for cascade control strategy.

As can be seen form Fig. 8, the reactor temperature has reached to its new desired value about 3 minutes. Variations of other controlled variables are shown in Fig. 9.

In another simulation, the desired value of the reactor pressure is increased by 1 bar. Fig. 10 shows variations of the reactor pressure and its related manipulated variables for cascade control strategy. Variations of other controlled variables are shown in Fig. 11.

As can be seen from Figs. 8 and 10, performances of reactor pressure and temperature control loops are fairly well for setpoint tracking and other control loops rejected the loads generated due to changes of the reactor pressure and temperature setpoints.

CONCLUSIONS

A two phase model including bubble and emulsion phases which considers bubble growth effect was used for modeling the hydrodynamic behavior of a fluidized bed polyethylene reactor. A double active sites Ziegler-Natta catalyst model was used for describing the kinetic of ethylene copolymerization. Using the balance equations and reaction kinetics, a software was developed for reactor dynamic simulation. Six control loops were considered for maintaining the reactor at the desired condition. Conventional PID controllers with anti-windup were used to control the reactor process variables. The performance of the control system was investigated for setpoint tracking and load rejection. It was shown that the control system can control the reactor operating conditions properly either for load rejection case or setpoint tracking. To improve the performance of the control system for load rejection, cascade control strategy was implemented.

Acknowledgments

The support of R and D of National Petrochemical Company is gratefully acknowledged.

Nomenclatures

A	Area, (cm^2)
A_{ex}	Heat transfer area of the heat exchanger, (cm^2)
a_c	Mole of active site per gram of catalyst, (mole/gr)
Cp	Specific heat, (J/g.K)
C	CoCatalyst
d	Diameter, (cm)
D	Dead polymer chain
dp	Particle diameter, (cm)
H	Bed height, (cm)
Hm	Overall heat transfer coefficient, ($J/k.s.cm^3$)
H_{bc}	Bubble-cloud hear transfer coefficient, ($J/k.s.cm^3$)
ΔH	Heat of reaction, (J/g)
ka	Kinetic rate constant of reactivation reaction, (s^{-1})
kd	Kinetic rate constant of deactivation reaction, (s^{-1})
kf	Kinetic rate constant of formation reaction, (cm^3/mole.s)
ki	Kinetic rate constant of initiation reaction, (cm^3/mole.s)
kp	Kinetic rate constant of propagation reaction, (cm^3/mole.s)
kt	Kinetic rate constant of chain transfer reaction, (cm^3/mole.s)

Km	Mass transfer coefficient, (s^{-1})
Kv	Valve coefficient
m	Total number of monomers
$\dot{m}$	Mass flow rate, (g/s)
[M]	Monomer concentration, ($mole/cm^3$)
$\overline{m}$	Average molecular weight of repeating unit in the polymer chain
MI	Melt flow index, (g/10 min)
$\overline{M}n$	Number-average molecular weight
Mw	Molecular weight, (g/mole)
$\overline{M}w$	Weight-average molecular weight
n	Total number of components
[N]	Active site concentration, ($mole/cm^3$)
$[N_2]$	Nitrogen concentration, ($mole/cm^3$)
P	Pressure, (bar)
PDI	Poly dispersity
PP	Partial pressure, (bar)
Q	Volumetric flow rate of polymer and gas mixture withdrawn from the reactor, (cm^3/s)
q	Mass flow rate, (g/s)
r	Polymer chain length
R_i	Consumption rate of molecular species, ($mole/s.cm^3$)
s	Total number of active sites
S_p	Potential active site
T	Temperature, (K)
U	Gas velocity, (cm/s)
U_{ex}	Overall heat transfer coefficient of the heat exchanger, ($J/k.s.cm^3$)
V	Volume, (cm^3)
Y	Total concentration of live polymer chain, ($mole/cm^3$)
X	Total concentration of dead polymer chain, ($mole/cm^3$)

Greek letters

α	Active site fraction
ε	Bed void fraction
ρ	Density (g/cm^3)
δ	Volumetric ratio of bubble phase to the bed volume
ϕ	Instantaneous polymer composition
Φ	Cumulative polymer composition

Superscripts and subscripts

av	Average
b	Bubble
cat	Catalyst
e	Emulsion
ex	Heat exchanger
g	Gas
in	Inlet
o	Outlet
p	Polymer
rec	Recycle
ref	Reference
w	Water

Received : 31st July 2007 ; Accepted : 23rd December 2007

REFERENCES

[1] Choi, K. Y., Ray, W. H., The Dynamic Behavior of Fluidized Bed Reactor for Solid Catalyzed Gas Phase Olefin Polymerization, *Chemical Engineering Science*, **40**, 2261 (1985).

[2] McAuley, K. B., Talbot, P., Harris, T. J., A Comparison of Two Phase and Well - Mixed Models for Fluidized Bed Polyethylene Reactors, *Chemical Engineering Science*, **49**, 2035 (1994).

[3] Hatzantonis, H., Yiannoulakis, H., Yiagopoulos, A., Kiparissides, C., Recent Developments in Modeling Gas-Phase Catalyzed Olefin Polymerization Fluidized Bed Reactors: The Effect of Bubble Size Variation on the Reactor Performance, *Chemical Engineering Science*, **55**, 3237 (2000).

[4] Kiashemshaki, A., Mostoufi, N., Sotudeh, R. Two-Phase Modeling of a Gas Phase Polyethylene Fluidized Bed Reactor, *Chemical Engineering Science,* **61**, 3997 (2006).

[5] McAulley, K. B., MacGregor, J. F., Hamielec, A. E., A Kinetic Model for Industrial Gas-Phase Ethylene Polymerization, *AIChE J.*, **36**, 837 (1990).

[6] Kunii, D., Levenspiel, O., "Fluidization Engineering", New York, Wiley (1990).

[7] Dadebo, S., Bell, M., Mclellan, P., Temperature Control of Industrial Gas Phase Polyethylene Reactors, *J. Process Control*, **7**, 83 (1997).

[8] Ali, E., Abasaeed, A., Al-Zahrani, S., Optimization and Control of Industrial Gas Phase Polyethylene Reactors, *Ind. Chem. Eng. Res.*, **37**, 3414 (1998).

[9] Seki, H., Ogawa, M., Ohshima, M., PID Temperature Control of an Unstable Gas-Phase Polyolefin Reactor, *J. Chem. Eng. Jpn.*, **34**, 1415 (2001).

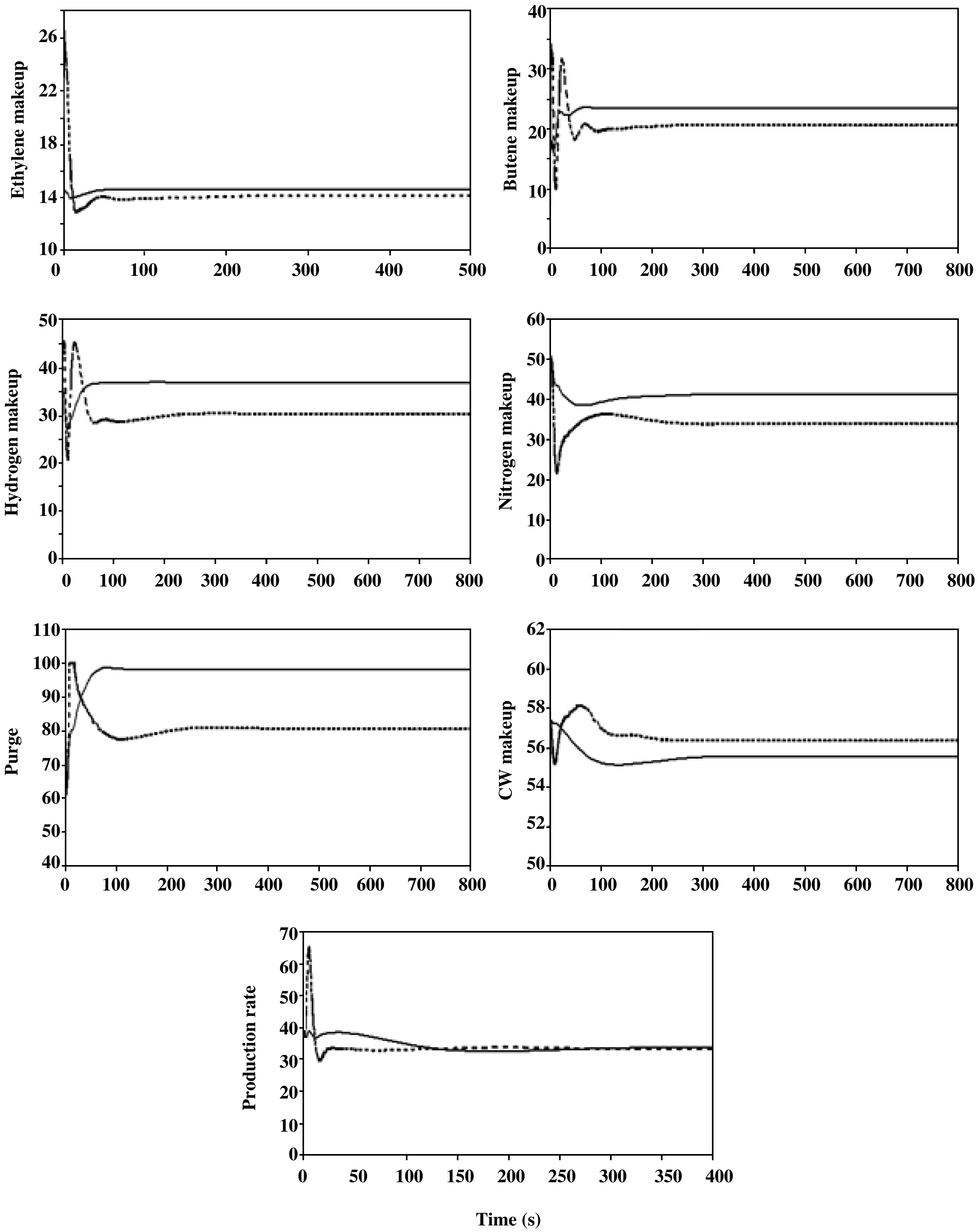

Fig. 5: Variations of manipulated variables (valve opening percentages) due to 5 bar increase in the makeup stream pressures (---- single concentration loops, —— cascade loops).

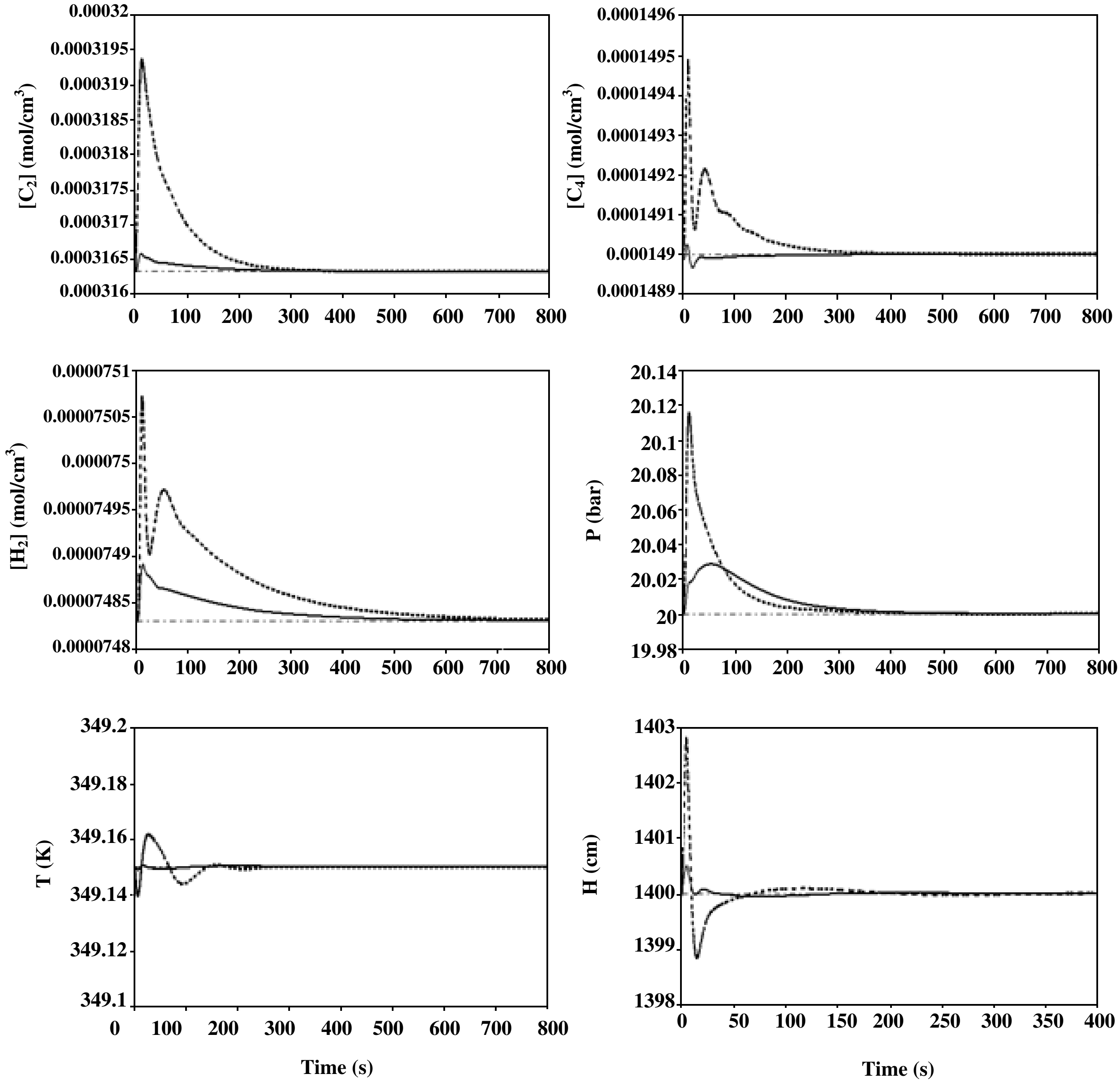

Fig. 6: Deviations of the controlled variables from their steady state values due to 5 bar increase in the makeup stream pressures under fixed purge flow rate(---- single concentration loops, —— cascade loops).

[10] McAuley, K. B., McGregor, J. F., Nonlinear Product Quality Control in Industrial Gas-Phase Polyethylene Reactor, *AICHE J.*, **39**, 855 (1993).

[11] Ali, E., Al-Humaizi K., Ajbar, A., Multivariable Control of Simulated Industrial Gas Phase Reactor, *Ind. Chem. Eng. Res.*, **42**, 2349 (2003).

[12] Chatzidoukas, C., Perkins, J. D., Pistikopoulos, E. N., Kiparissides, C., Optimal Grade Transition and Selection of Closed Loop Controllers in a Gas Phase Olefin Polymerization Fluidized Bed Reactor, *Chemical Engineering Science*, **58**, 3543 (2003).

[13] Bequette, W., "Process Control, Modeling, Design and Simulation", Prentice Hall, (2003).

[14] Luyben, W. L., Simple Method for Tuning SISO Controllers in a Multivariable System, *Ind, Eng. Chem. Proc. Des. Dev.*, **25**, 654 (1986).

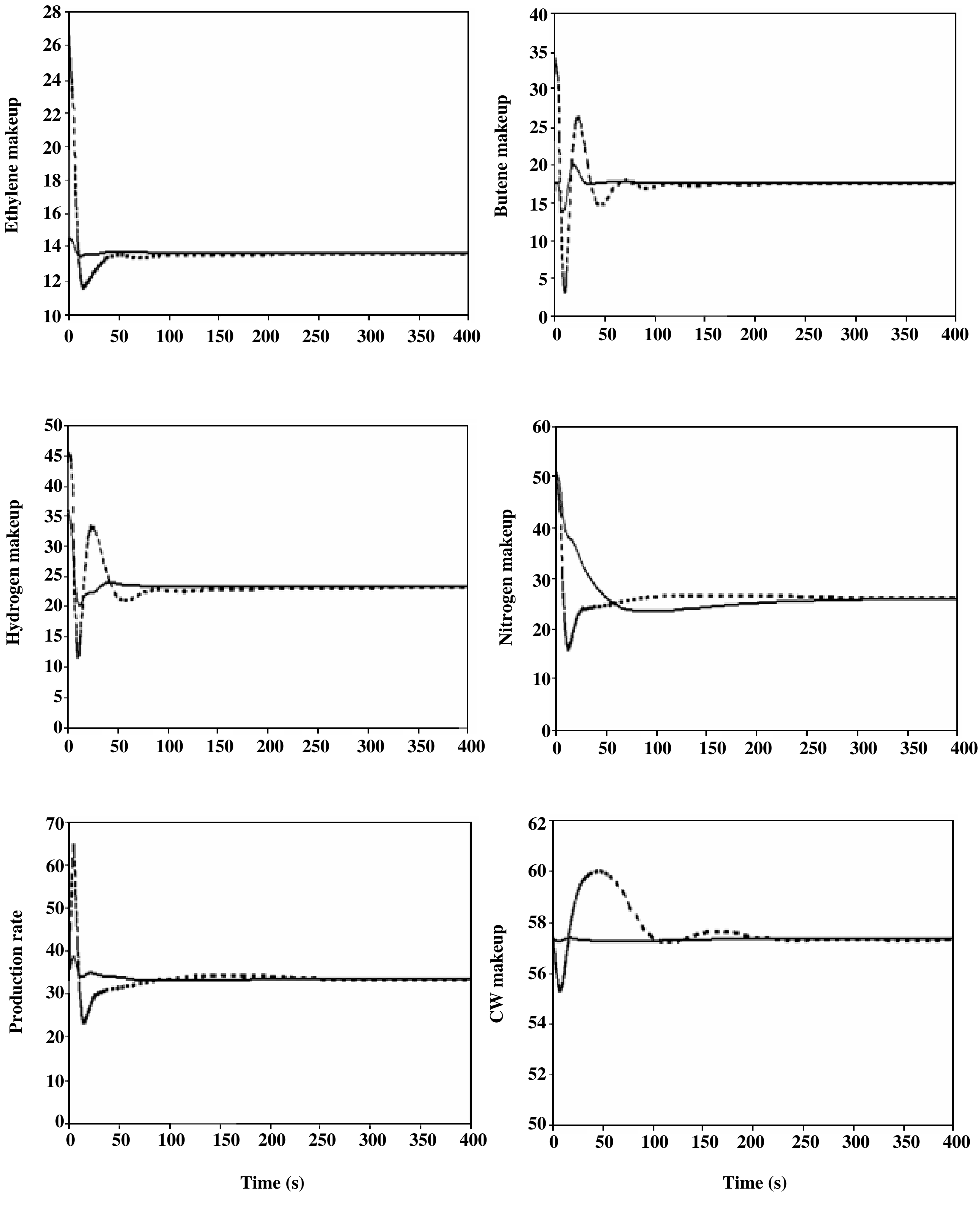

Fig. 7: Variations of manipulated variables (valve opening percentages) due to 5 bar increase in the makeup stream pressures under fixed purge flow rate (---- single concentration loops, —— cascade loops).

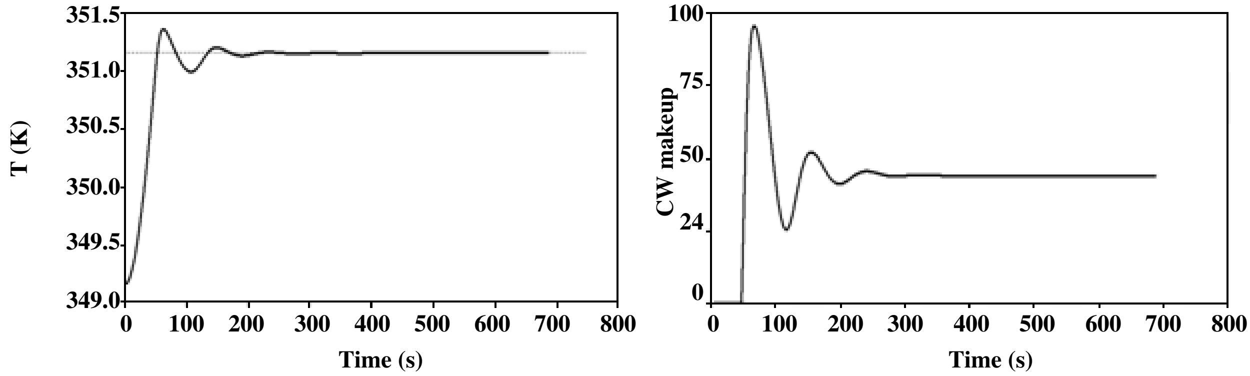

Fig. 8: Variations of the reactor temperature and cooling water makeup stream (valve opening percentage) due to 2 °C increase in the reactor temperature setpoint.

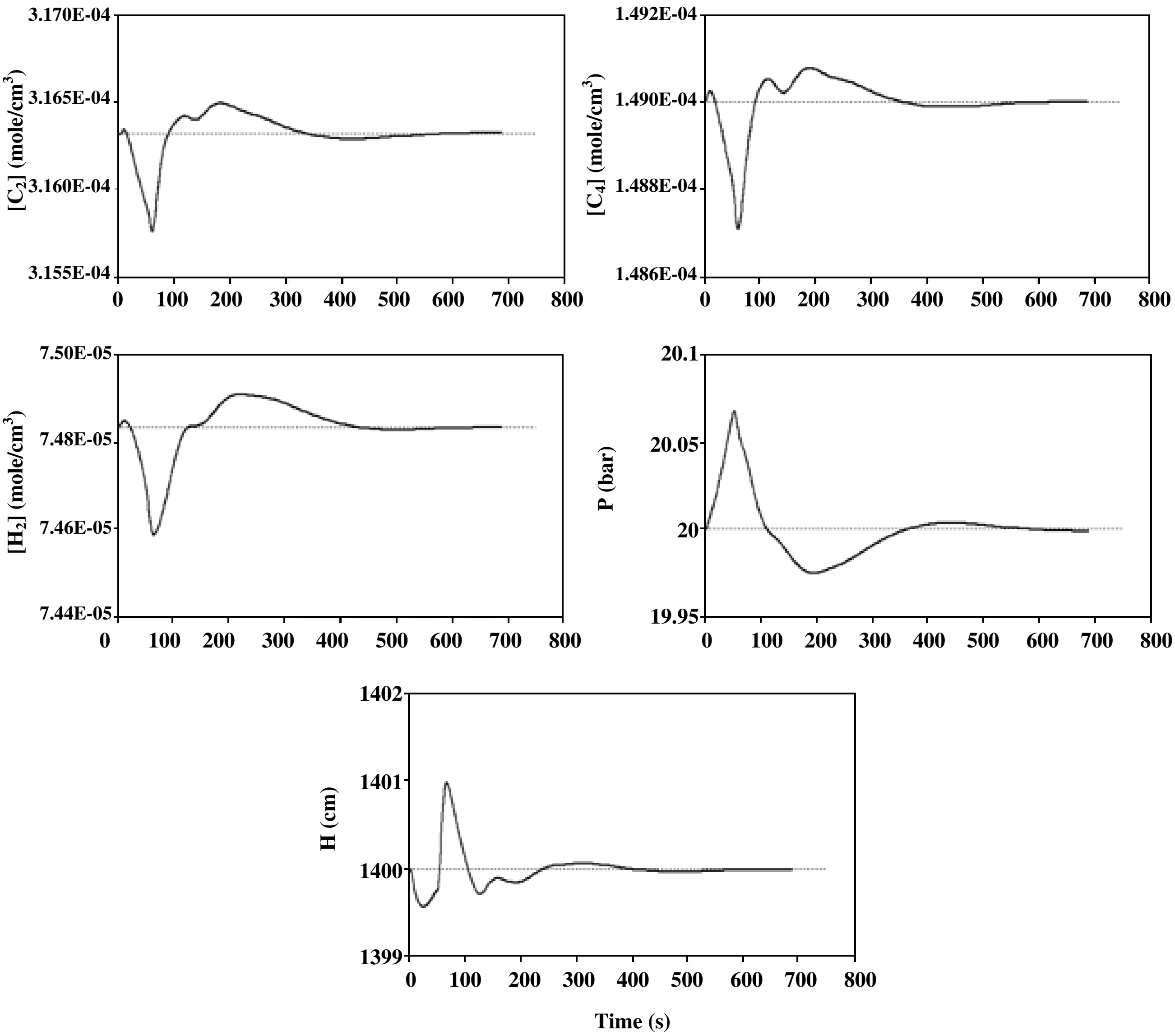

Fig. 9: Variations of other controlled variables due to 2 °C increase in the reactor temperature setpoint.

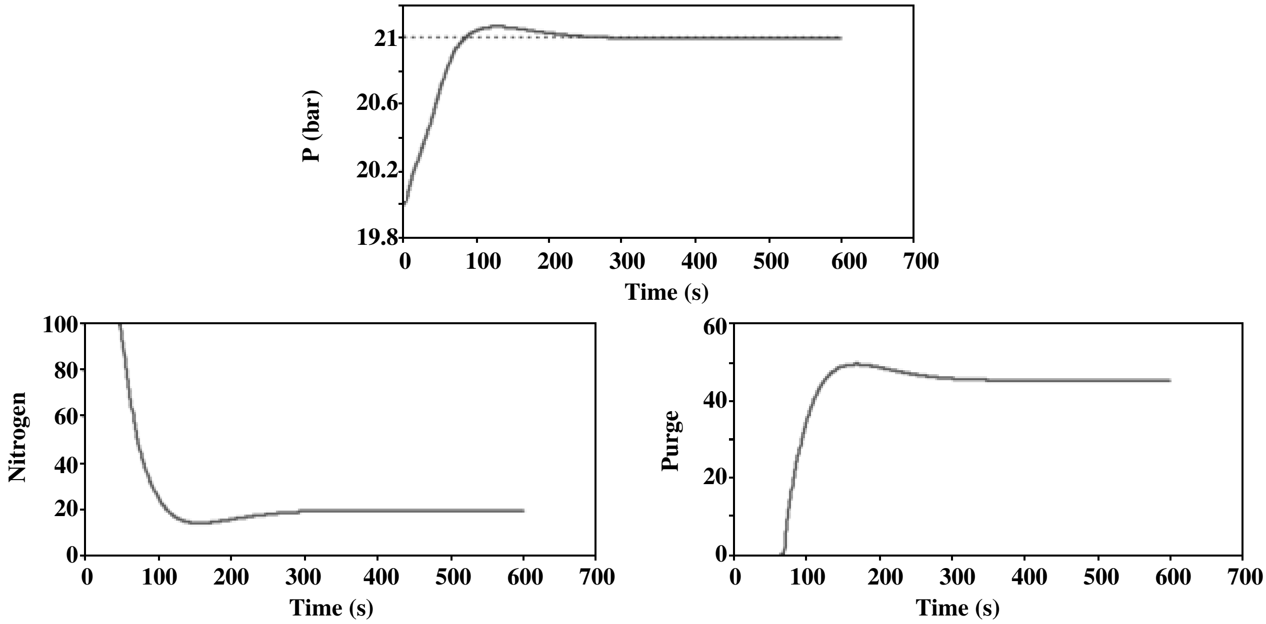

Fig. 10: Variations of the reactor pressure and the nitrogen and purge volumetric flow rates (valve opening percentages) due to 1 bar increase in the reactor pressure setpoint.

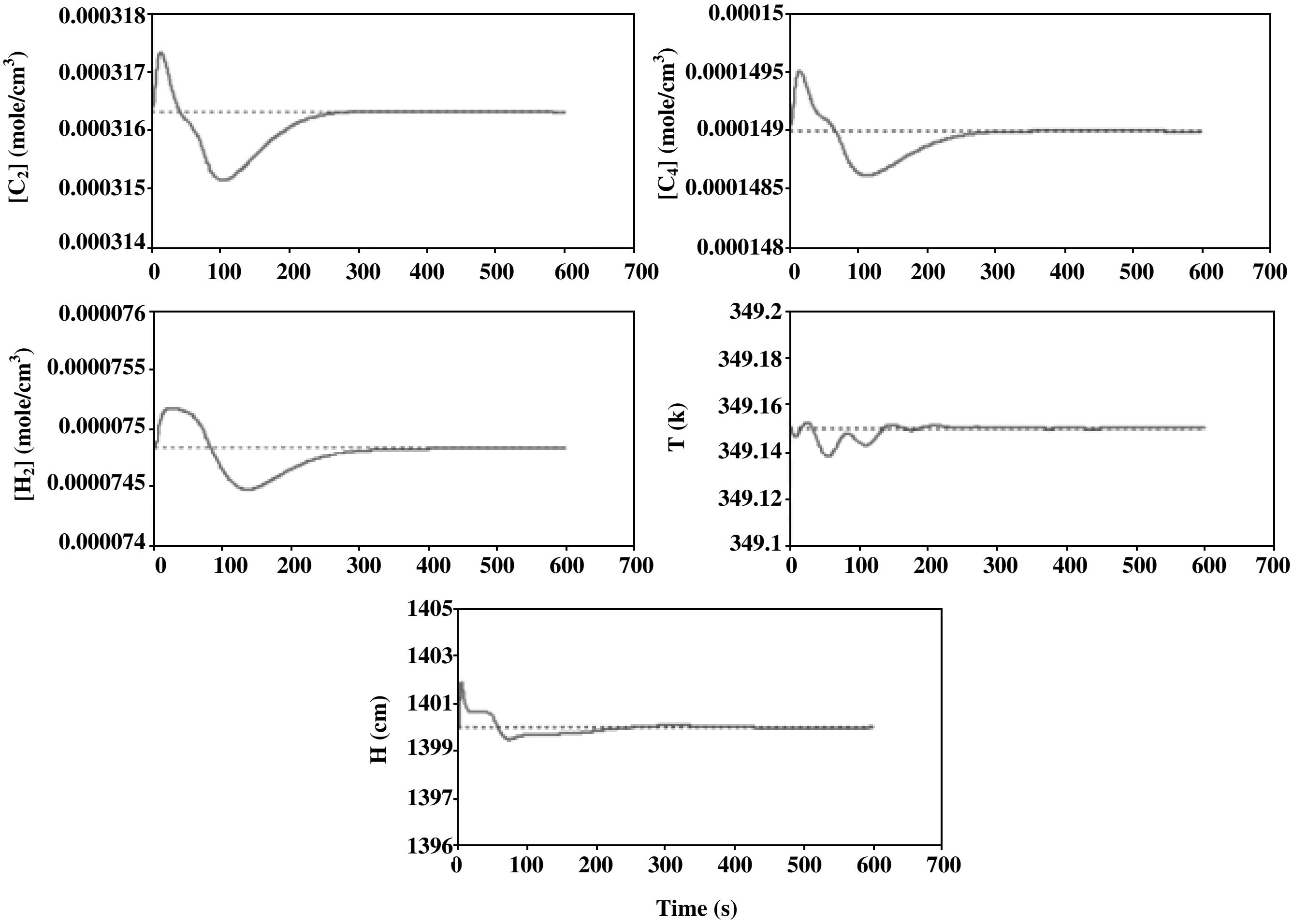

Fig. 11: Variations of other controlled variables due to 1 bar increase in the reactor pressure setpoint.